Hindawi
Journal of Nanomaterials
Volume 2021, Article ID 9236530, 10 pages
https://doi.org/10.1155/2021/9236530

Research Article

Electrochemical Anodic Synthesis and Analysis of TiO_2 Nanotubes for Biomedical Applications

V. Sivaprakash,[1] **L. Natrayan**,[2] **R. Suryanarayanan**,[1] **R. Narayanan**,[1] **and Prabhu Paramasivam**[3]

[1]*School of Mechanical Engineering, Vellore Institute of Technology, Chennai, 600127 Tamil Nadu, India*
[2]*-Department of Mechanical Engineering, Saveetha School of Engineering, SIMATS, Chennai, 602105 Tamil Nadu, India*
[3]*Department of Mechanical Engineering, College of Engineering and Technology, Mettu University, Ethiopia -318*

Correspondence should be addressed to R. Narayanan; rnarayann69@gmail.com
and Prabhu Paramasivam; prabhu.paramasivam@meu.edu.et

Received 13 July 2021; Revised 15 September 2021; Accepted 18 September 2021; Published 30 September 2021

Academic Editor: Vidyadhar Singh

Nowadays, titanium and alloy materials are encouraged for biomedical applications. Fabrication of the passive layer over the titanium materials is limited. Typically, a plain titanium sample is not suitable for bioimplant applications because the adhesion of biological elements like blood cells, tissues, and bones is poor. The use of surface-modified titanium resolves this issue. Surface modifications on titanium by electrochemical methods are simple and cost-effective. The addition of water to the ethylene-based electrolyte-enhanced the oxidation process to increase the length of the nanotubes. Surface morphological analysis shows that the length of the nanotubes has been increased, nanoindentation analysis delivers that increasing the length has been increased the hardness level, and corrosion analysis indicates that the length of nanotubes encouraged the corrosion resistance. Potentiodynamic polarization, Bode and Nyquist plots were models fit analyzed with equivalent electrical circuits. Sample cell viability was characterized with NIH-3T3 cells using an inverted microscopy analyzer.

1. Introduction

Recently, biomedical device fabrication processes have been gaining significant attention from researchers. Titanium alloys are best suited to fabricate biomedical implants as they possess good adaptability in the biological environment. However, the material in as received condition possesses poor biocompatibility characteristics, making it lethal to the human body [1]. For enhanced bioadaptability of the Ti alloy with toxicity behaviour, the surface needs to be modified. Different techniques are available for material surface modification like physical vapour deposition, chemical vapour deposition, sol-gel, hydrothermal, and electrochemical anodization. From the techniques mentioned above, the electrochemical anodization is the easiest and feasible technique for surface modification. Compared to other techniques, electrochemical anodization needs a simple working setup that consumes low space and energy to fabricate the stable and compact TiO_2 nanotubes on the surface of the Ti foil [2]. In the anodization process, the presence of the ion particles in the electrolyte provides continuous etching according to the theory of field-assisted dissolution, resulting in the oxide layers formed over the nanotubes [3]. The fluorine-based electrolytes were observed to produce better etching, according to Zwilling et al. 1999 [4]. Gong et al. 2001 [5] introduced vertical oriented hydrofluoric-based electrolyte to fabricate the TiO_2 nanotubes [4]. The researchers [1–4] found that nanotube geometrical performances have been varied by electrolyte concentration. NH_4F, sodium sulfate, H_2PO_4, $(NH_4)_2SO_4$ [6], H_3PO_4, ethylene glycol, glycerol, and various electrolyte combinations were utilized to fabricate the TiO_2 nanotubes. Processing time was reported to have a strong influence on the anodization process [7]. The geometrical properties have been improved with the control of the anodization time and potential of the electrolyte [8]. Temperature maintenance in

electrolytes delivers a good result. Pishkar et al. deliver a report on electrolyte temperature at ~20°C with various input potentials deliver the length of the nanotube around 7 μm at various input conditions, water content, and anodization time [9]. In addition, the effect of electrolyte-water content presences also plays a major role in the anodization process. Sreekantan et al. 2011 showed the use of varying input parameters like voltage and time in 15% of water content electrolytes produced nanotubes ~17 μm length. From these results, it is concluded that water content in electrolytes influenced the length of nanotubes. From another analysis, the water content around 5 vol. % delivers the length of 6.69 μm could be identified at 50 V of input potential [11]. Sometimes, the overdose of water content may be strongly disagreed with because the maximized water contents are not suitable for the nanotube growth [12]. A suitable level of water contents highly encouraged the growth rate of nanotube formation on the materials was identified [13]. The nanotube formation with high water content on the electrolyte, the rib formation [14] could be identified. Moreover, these rib formations are encouraging the hardness values were reported.

The need to increase the length of nanotubes is to achieve enough cell attachment with the bone and related areas, which are only in direct contact with the compact surface layer. The morphology of the nanotubes formed was highly affected by the water content % in the electrolyte, as the variation in the water content determined the dissolution of F^- and H^+ ions during the anodization process [15]. The initial delay in the addition of varying water content % in the electrolyte affects the electrochemical kinetics during the electrochemical anodization process. Therefore, the samples fabricated under different water content percentages with delayed addition were analyzed for the surface morphological behaviour. For this reason, the prime focus is given on the length of the nanotubes. The novelty of this research is to increase the length of the nanotubes by increasing the water content in the ethylene glycol electrolyte after 5 minutes of anodization. In addition, the nanotube surface morphologies were analyzed by high-resolution scanning electron microscope (HR-SEM), nanomechanical properties were analyzed by nanoindentation, and corrosion behaviour was studied with the use of Gamry instruments cell viability was characterized by an inverted microscope analyzer.

2. Materials and Methods

Commercially pure titanium was used to fabricate the TiO_2 nanotubes. Titanium plates of 20 ∗ 35 mm 1 mm thickness were prepared for anodization by polishing the sample with the assistance of 180, 400, 800, and 1500 grid size papers to obtain mirror-like polish. The mirror-like structure has been etched with 1, 4, and 5% hydrofluoric acid, nitric acid, and water content for a 30 s etching period. The etched sample was cleaned with distilled water to remove the poisonous content over the material and dried with hot air for 60 s. The prepared sample was sealed with cellophane tape in the unetched area. SBF (simulated body fluid) solution was prepared with the following regents NaCl 80.35, $NaHCO_3$ 0.355, KCl 0.225, $K_2HPO_4.3H_2O$ 0.231, $MgCl_2.6H_2O$ 0.311, $CaCl_2$ 0.292, Na_2SO_4 0.072, and Tris buffer solution 6.118 g (if pH values less than 7.4) then HCl used to increase the pH value above 7.45.

The prepared sample was connected with an anode terminal, and the cathode terminal was connected with the platinum wire of 1 mm diameter. Both the anode and cathode were dipped in an electrolyte containing ethylene glycol, NH_4F (0.5 wt%) without water. Input potential was selected as 30 V for 1 hour of anodization period, after 5 minutes of the experiment, 10 vol. % of water was added till the rest of the experiment was completed. In another experiment, 20 vol. % water was added after 5 minutes after the experiments started. Post the anodization process; the samples were subjected to heat treatment at 600°C for 1 hr for phase conversion. The different phases in the synthesized nanotubes were identified using XRD. The in vitro analysis for the cell toxicity was conducted with the help of MTT (2, 3-bis-(2-methoxy–4–nitro–5–sulfophenyl)-2H–tetrazolium–5-carboxamide), which is a yellow colour salt, that is metabolized by living cells into nicotinamide adenine dinucleotide (NADH) and nicotinamide adenine dinucleotide phosphate (NADPH). MTT assay is the widely employed method to determine cell culture viability after incubation of a drug for a stipulated time. When yellow colour MTT is added to the culture, the viable cells convert the yellow salt to purple colour formazan crystals. These purple formazan crystals could be solubilized using dimethyl sulfoxide (DMSO) to read the absorbance at 595 nm using an absorbance reader.

3. Results and Discussion

HRSEM, XRD, and nanoindentation techniques characterized anodized TiO_2 nanotubes. The surface morphological analysis by HRSEM showed the formation of top, open, and bottom closed cylindrical types of nanotubes. The mechanical properties of nanotubes were identified with a nanoindentation analyzer. Berkovich nanoindentation tip was used to characterize the nanotube hardness, contact depth, and elastic modulus of the nanotubes have been identified. H indicated the hardness value of the nanotubes and $H = P_{\max}/A$. $P_{\max}$ is the maximum load applied to the material, and A indicates the contact area between the indenter to the nanotubes. The area to the nanoindenter, A is presented in equation (1). S stiffness coefficient is shown in equation (2)

$$A = \sqrt[3]{3h_f^2}\ \tan^2 65.3 = 23.69h_f^2, \quad (1)$$

where $h_f = h_{\max} = -\varepsilon P_{\max}/S$.

S indicates the stiffness coefficient of unloading curves.

$$S = \left(\frac{\partial p}{\partial h}\right) h = h_{\max}. \quad (2)$$

Corrosion analysis of TiO_2 nanotubes was analyzed by Gamry instrument 1010 interface. The kinetic behaviour of the nanotube was characterized with the help of the SBF

solution. The solution was prepared and used within 24 hours after preparation. The potentiodynamic polarization studies were used to analyze the corrosion behaviour of nanotubes and bode plots, and Nyquist plots were used to analyze the kinetic behaviour of nanotubes. Equivalent electrical circuits (EES) were modelled to fit with the bode plots. The NIH -3T3 cells were utilized to identify the cell viability of the TiO_2 nanotubes.

3.1. Surface Morphological Analysis. Commercially pure titanium has been used to fabricate the TiO_2 nanotubes. The HR-SEM analysis identified different surface morphological results. Figure 1(a) shows the nanotubes fabricated under 10 vol. % of water content. The nanotube surface morphology indicates that the rib structure has been formed in the initial section due to the water content added to the electrolyte. The same scenario is also observed in the sample fabricated at 20 vol. % of water contents. The nanotube all over rib structures could be achieved as shown in Figure 1(b). The tube top layers showed the self-organized nanotubes are shown in Figure 1(c). The tube growth has been varied. The ups and down layers have been identified from Figures 1(c) and 1(d). The even formation that has been slightly modified in the presence of water contents shows the water content has varied the formation of nanotubes. The tube diameter and length variation are due to the increased oxidation (O_2 or OH- ions) due to the high water content, which is explained by the following chemical reactions occurring during the anodization process [15].

$$\begin{aligned}&\text{Electrochemical reaction on the water, } 2H_2O \text{—>} O_2 + 4e^- + 4H^+,\\&\text{Produced } O_2 \text{ reacts with Ti to form } TiO_2,\ Ti + O_2 \text{—>} TiO_2.\end{aligned} \tag{3}$$

The dissolution of the Ti ions in the electrolyte solution at the metal and oxide interface under the electric field is presented as

$$\text{Ti}\,4{+}{+}6\,\text{F} - \text{—} > \text{TiF}62-. \tag{4}$$

The synthesis of TiO2 nanotubes on the Ti foil through anodization is presented as

$$TiF_6^{2-} + 2\,H_2O \text{—>} TiO_2 + 6\,F^- + 4H^+. \tag{5}$$

The fluorine ions observed in equations (4) and (5) result in forming the pitting of the oxide layer. The tubes formed due to the pitting action were observed to dissolve into the oxide layer chemically. The variations in the dimensions of the formed tubes indicate the influence of increased H_2O concentration, which determined the dissolution rate of F^- and H^+ ions. As a result, due to the increased dissolution of F^- and H^+ ions with the high water content %, the growth of the nanotubes increased [16, 17].

Furthermore, various factors can also affect the formation of TiO_2 nanotubes. There are different combinations of possibilities that assist in forming self-organized nanotubes on titanium surface by electrolyte containing ethylene glycol, ammonium fluoride and water content %, electrolyte temperature, and input potential anodization time [18–20].

3.2. XRD Analysis. The crystalline phase transformation has been analyzed by X-ray diffraction. The water involved anodized samples were heat-treated up to 600°C. The diffraction peaks were found in 38.39, 40.16, 52.92, 62.88, and 70.63° major for titanium phases. 25.26° for the amorphous and rutile phases were identified as follows 27.46, 54.33, and 56.72° were identified. However, the plain titanium sample indicates the absence of amorphous and rutile phases shown in Figure 2(a). After anodized the sample involved to heat treatment to 450°C, the sample's phases indicated that the amorphous peak was noted as (A), and the amorphous phases were brittle and weak. Further heat treatment, the amorphous phases is converted to a crystalline structure. About 550°C, the samples indicated the mixed amorphous and crystalline phases shown in Figure 2(b). Furthermore, increased heat in the samples indicated highly crystalline phases, identified in Figure 2(c).

3.3. Nanomechanical Property Analysis. The mechanical properties of the TiO_2 nanotubes fabricated in the water adding method are shown in Figure 3. The plain anodized samples were shown in sample 1 and sample 2. The anodized samples are amorphous and weak in phase structure. The molecular bonding was weak. After annealing temperature (sample 3 and sample 4), the weak amorphous structure has been converted to solid crystalline structures. After the phase conversion, the samples showed increased hardness values from 648, 648.71, 649, and 650.25 nm. The nanoindentation experiments start at zero (point an in Figure 2) indicating zero load. After increasing the load, the graph gradually increased 50 μN/sec to point (b) at a maximum load of 9000 μN. Then, the load is held for few seconds to point (c). Post the dwell period; the load is decreased to point (d) at the rate of 100 μN/sec. The straight line indicates that the sample is in plastic behaviour of superplasticity behaviour.

3.4. Corrosion Analysis. In this section, the corrosion behaviour of TiO_2 nanotubes fabricated in the water addition method was analyzed. The Gamry 1010 interface with SBF medium was utilized to analyze the behaviour was characterized. Every time, a fresh SBF was prepared and used for this analysis. Anodized samples were connected with the positive terminal, the platinum wire was connected with the negative terminal, and calomel was used as a reference electrode. The potentiodynamic study was analysis conducted between -0.5 and 5 mv.

3.5. Potentiodynamic Polarization. Corrosion occurs based on the direct chemical reaction on the surface of the material. Figure 3 represents the polarization study of the plain sample (1), TiO_2 nanotubes fabricated with 10 vol.% of water added (10 vol. % (2), 20 vol.% (3)) condition after 5 minutes of anodization starts. These curves evaded that corrosion current density has been decreased and potential values get increased. This current density and potential changes indicated that corrosion resistivity has increased due to the passivation layer (TiO_2) oxide layer. Table 1 represents the

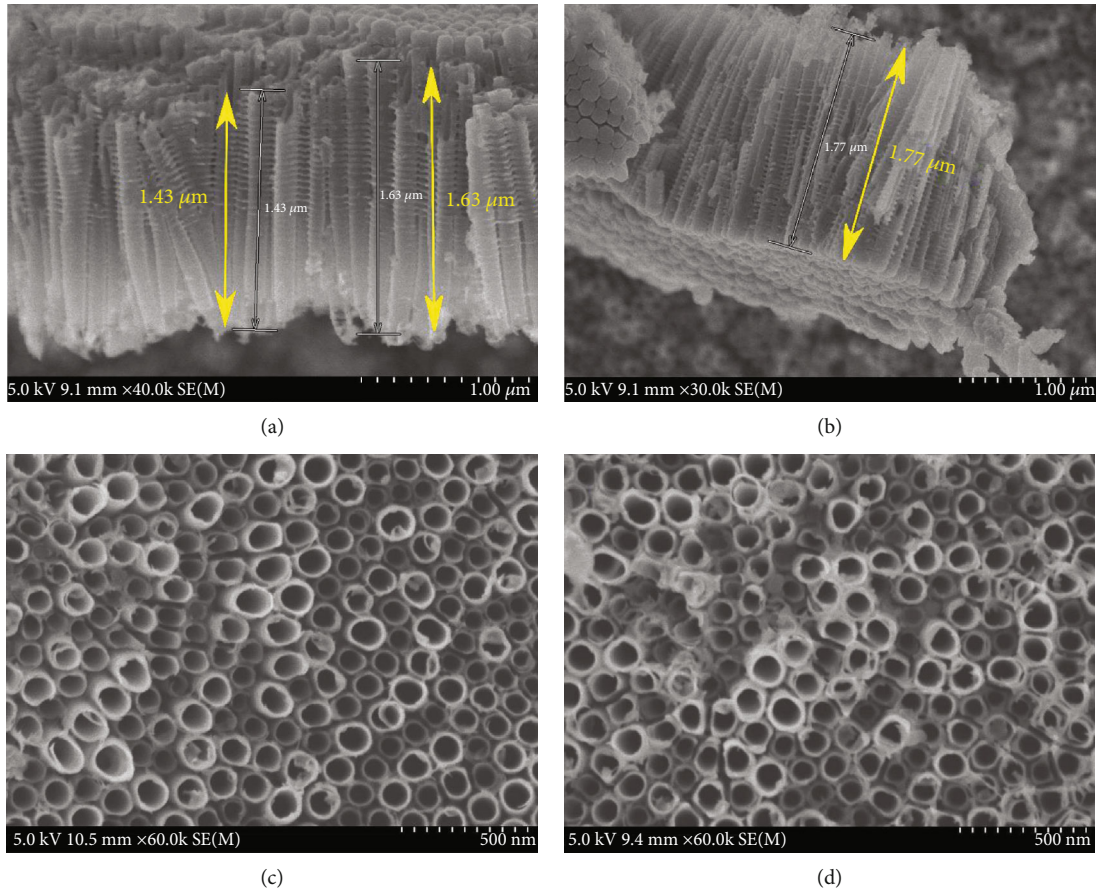

Figure 1: Surface morphological analysis of TiO_2 nanotubes fabricated with the use of water drop analysis.

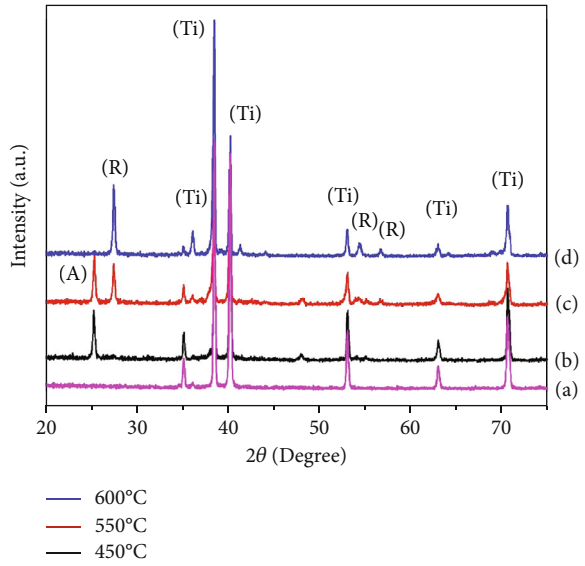

Figure 2: TiO_2 nanotubes phase change analysis by XRD.

E_{corr} and i_{corr} values that were changed due to the passivation layer thickness increment. The polarization curves start from the active region (-0.5 mV) to the passive region (+ 4 mV), which is the standard measurement method of this type of sample [21]. The cathodic reaction is nothing but the gain of electrons from the environment to the material. The anodic reaction loses the electrons from material to environment. A solution containing dissolved ions capable of carrying electricity is known as an electrolyte. An aqueous solution, or water with dissolved ions, is the most common electrolyte, although other liquids, such as liquid ammonia, may also be used.

The highest current density indicates the highest dissolution rate. From the base of dissolution rate, the plain nonanodized sample has a back lack of corrosion resistivity; on the other hand, the anodized samples inform the highest corrosion rate. This visual identification is confirmed by the measurement shown in Table 1. The E_{corr} and I_{corr} values for samples are as follows: E_{corr} for plain samples receives 0.122 and 0.466, and 0.455 mV was reached in the anodized sample.

3.6. Electrochemical Impedance Spectroscopy (EIS) Investigations. The bode, phase angle, and Nyquist plots were shown in Figure 4 after immersion of 30 minutes in SBF solution. According to electrochemical theory, a current flow may also be obtained by charging and discharging the double layer at the interface or by oxidizing/reducing chemicals on the electrode or in solution [22, 23]. The fitting model for the EIS analysis equivalent electrical simple model circuit (two times constant) is shown in Figure 4(c) as EEC.

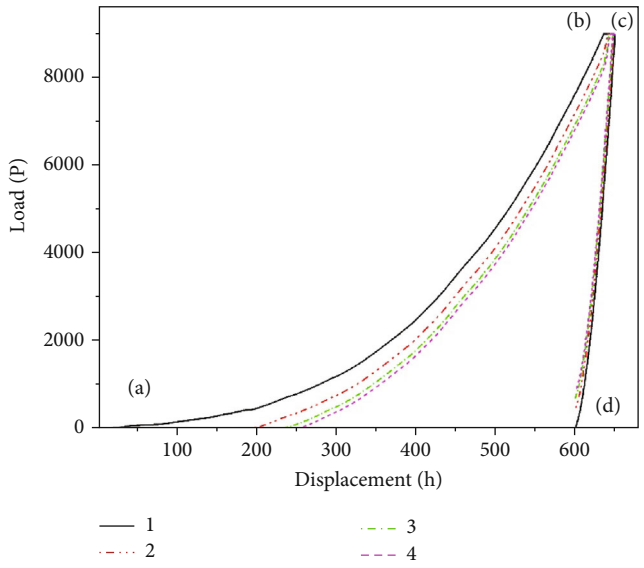

Figure 3: Nanomechanical properties of TiO_2 nanotubes fabricated underwater adding condition.

Table 1: Corrosion parameters calculation in SBF solution, anodization of TiO_2 nanotubes in water pour method.

	E_{corr}	i_{Corr}	Bc	Ba
Plain sample	0.122	-1.176	-0.456	1.972
Sample 1	0.466	-2.384	-0.281	2.35
Sample 2	0.455	-2.98	-0.274	2.131

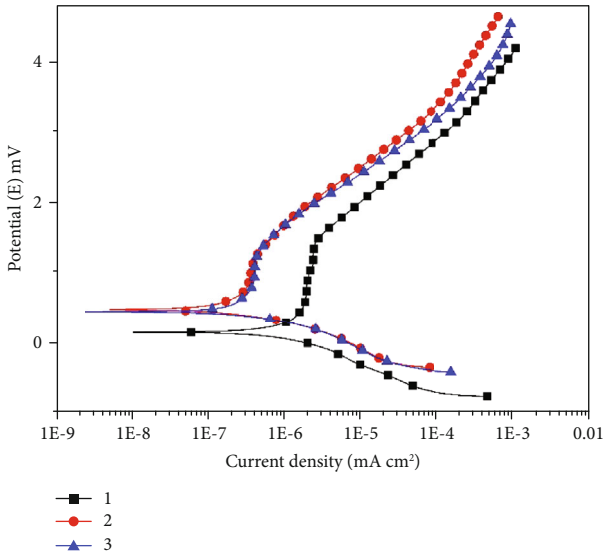

Figure 4: Potentiodynamic polarization study of TiO_2 nanotubes fabricated in water pour method.

This method directly connects impedance and phase angle measurements as frequency, voltage, or current functions. The stimulus is a low-amplitude alternating current signal used to detect the electric field or potential difference between various sections of the sample.

Table 2: EIS parameter results obtained from plain, 10 vol.% and 20 vol. % of water contents.

	Plain sample	10 vol.%	20 vol.%
Rs (Ω cm^2)	170.6	171.4	171.8
CPE_1 (F cm^2)	$7.93E-06$	$7.88E-06$	$2.54E-05$
$n1$	$9.45E-01$	$9.39E-01$	$9.96E-01$
Rc (Ω cm^2)	$3.16E+03$	$4.85E+03$	$1.90E+03$
Rb (Ω cm^2)	931.9	$1.18E+03$	$1.38E+04$
CPE_2 (F cm^2)	$5.10E-04$	$2.81E-04$	$1.02E-05$
$n2$	$7.80E-01$	$8.34E-01$	$9.23E-01$
Goodness of fit	$5.87E-04$	$3.44E-04$	$5.43E-05$

The impedance spectrum of the samples examined is determined by the connection between the data of the applied stimulus and the response obtained as a function of frequency [24, 25]. The kinetic behaviour results achieved in the EEC model are listed in Table 2. Here, Rs represents solution resistance, CPE_1 denotes the double layer capacitance, Rc represents charge transfer resistance, and CPE_2 is noted as coating capacitance. Rb refers to coating resistances [26, 27], and n denotes the phase shift to porous layers [28].

Figure 5(a) represents the impedance graph for the various anodized conditions. The frequency of the samples was increased when the nanotubes fabricated water content varied. The plain sample and 10 vol. % sample show similar results; on the other hand, the 20 vol.% of water contents frequency results were comparatively increased. This change of frequency may be the rib formation all over the nanotubes at the high-frequency results. An increase in frequency level can also be due to the absorption by nanotubes; ingredients present in the SBF solution take a high electrical resistance [21].

The phase angle shows that the plain sample delivers a low level of angle. After the water content is added to the solution result, the 10 vol. % of water addition increases the phase angle compared to the plain sample, and the 20 vol. % of water content sample delivers the maximized result could be identified from Figure 5(b). This increment in phase angle may be the reason for the increase in tube surface morphology. The increase in rib structure over the tube morphology may resist the kinetic behaviour of the nanotube or passive layer. Assumption of increment in phase angle also indicates that the passive layer's high stability occurs due to the nanotubes rib formation.

Nyquist plot represented in Figure 4(c) the charge transfer between the electrode, and the electrolyte is typically represented by a semicircular arc in conventional electrode materials [29]. The existence of one half-circle shows that the system has an electrochemical interface. On the horizontal and vertical axes, respectively, Nyquist displays the complex impedance's real and negative imaginary components [30]. The plain uncoated refers to lower surface resistance and the nanotube fabricated under 10 vol. % and 20 vol. % indicated the higher resistance compared to the plain sample. This increment happens by the formation of

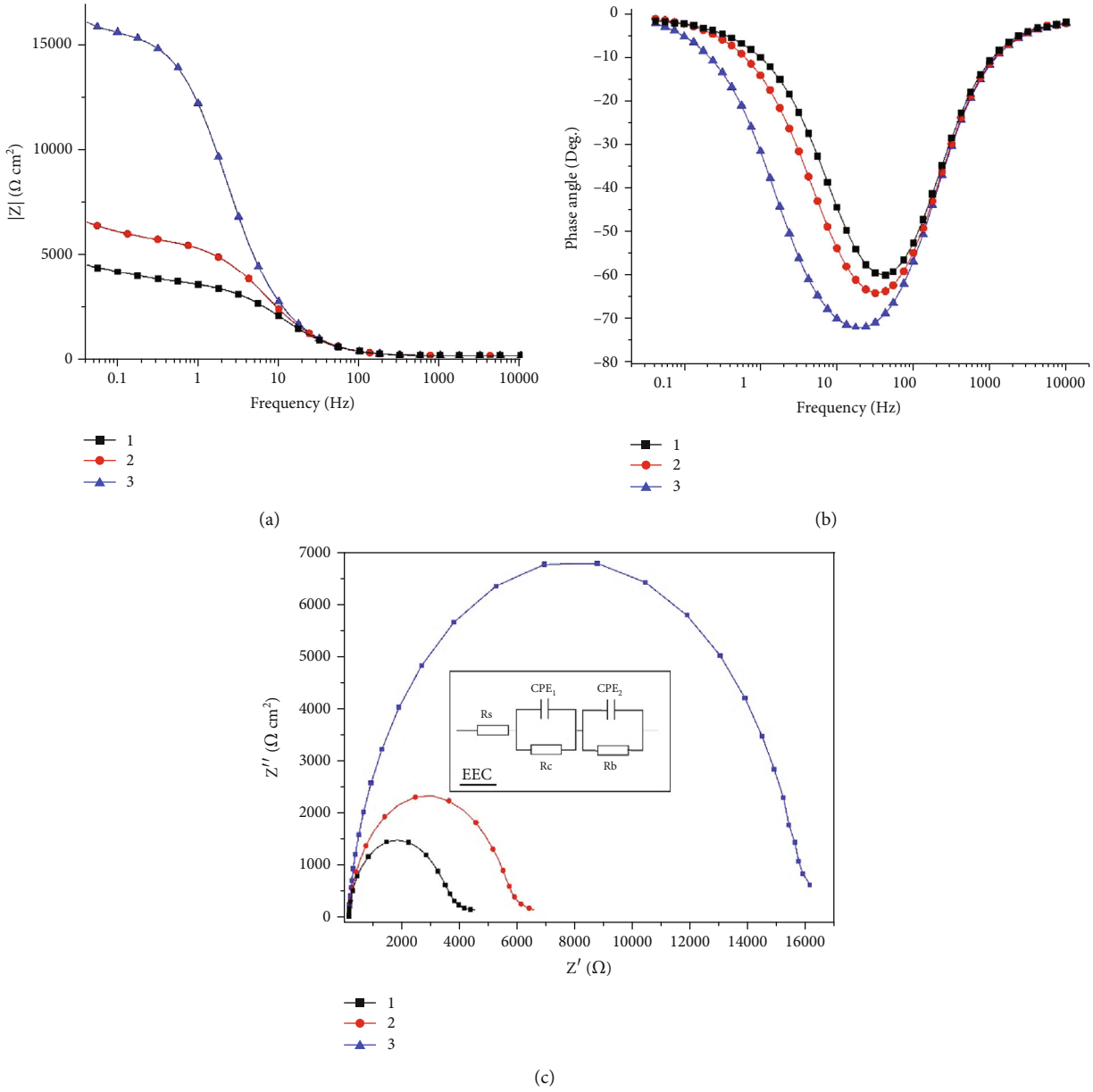

Figure 5: Kinetic behaviour analysis of TiO_2 nanotubes: (a) bode, (b) phase angle and Nyquist plots.

nanotubes over the material. The nanotube has resisted the resistivity by the solution to the sample.

On the other hand, the higher resistivity sample increased may be the formation of ribs over the entire surface of nanotubes. In Table 2, the solution resistance increased to 170.6, 171.4, and 171.8 for the plain, 10 vol. % and 20 vol. % of water content fabricated conditions.

3.7. In Vitro Analysis. NIH 3T3 cells were used to analyze the toxicity of titanium oxide nanotubes fabricated under different water vol. %. The analysis is carried out at three different incubation times of 24, 48, and 72 hours. MTT is the yellow salt that is metabolized by live cells in NADH (nicotinamide adenine dinucleotide) and NADPH (nicotinamide adenine dinucleotide phosphate) and (3-(4, 5-dimethylthiazol-2)-2, 5-diphenyltetrazuolium bromide). The control cells were shown in Figure 5 with incubation time for 24 (Figure 6(a)), 48 (Figure 6(b)), and 72 hours (Figure 6(c)), respectively. At 24 hours of control samples shown, a less amount of cell was spread in the empty wee, 48 hours shown cell growth was increased, and 72 hours of incubation show the high growth of cell was shown in Figure 5(c). The cell viability for both the 10 and 20 vol. % of samples indicates the same morphology shown in Figure 5(d).

Moreover, 48 hours of incubation time sample were indicated in Figures 6(e) and 6(f). The cell growth was highly increased, which could be identified from the inverted microscopically images. The sample encourages the cell viability on the surface area indicated the samples were nontoxicity after 24 to 48 hours. Above the incubation time of 48 hours, the test results were analyzed at 72 hours of incubation. Figures 6(g) and 6(h) inform that the cell growth

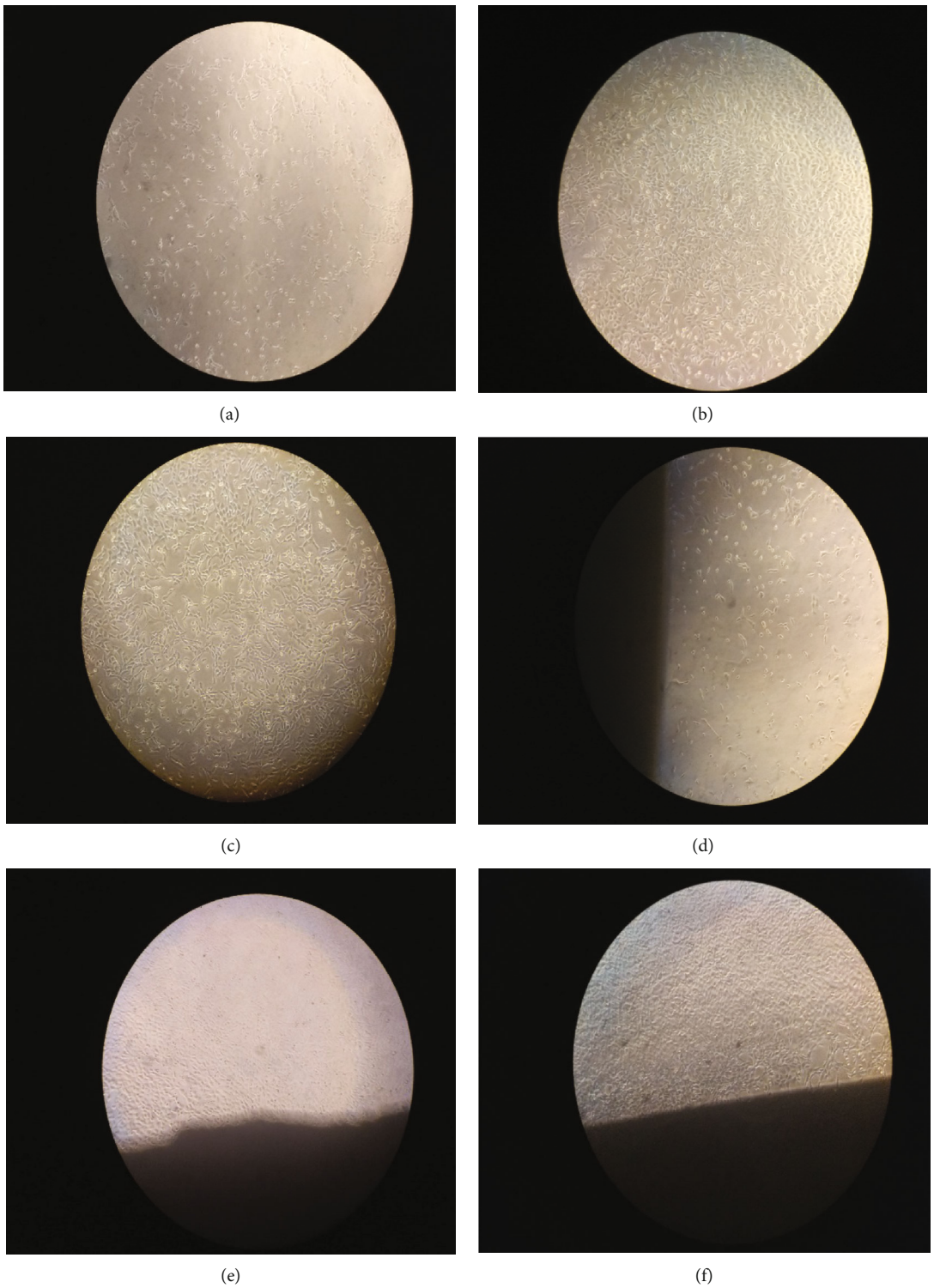

(a) (b) (c) (d) (e) (f)

Figure 6: Continued.

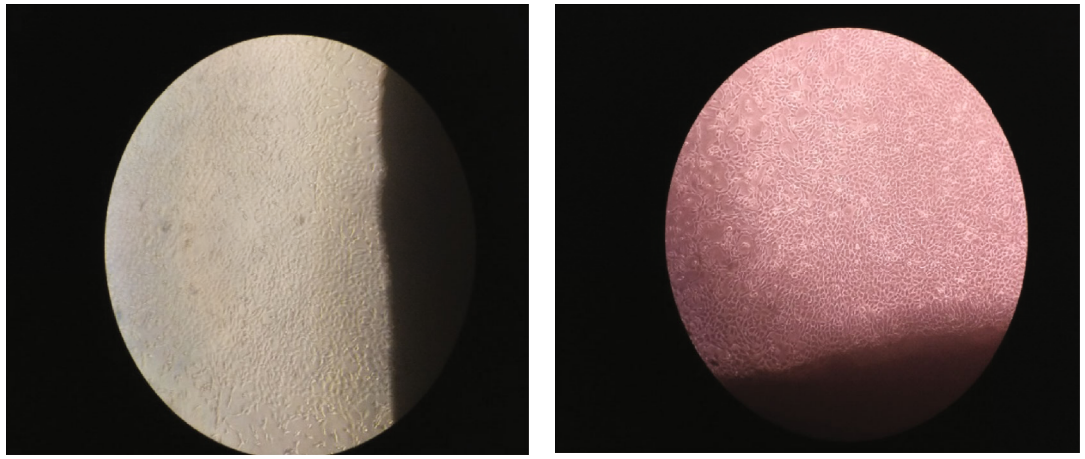

(g) (h)

Figure 6: Cell viability analysis of TiO_2 nanotubes fabricated under 10 and 20 vol. % of water content.

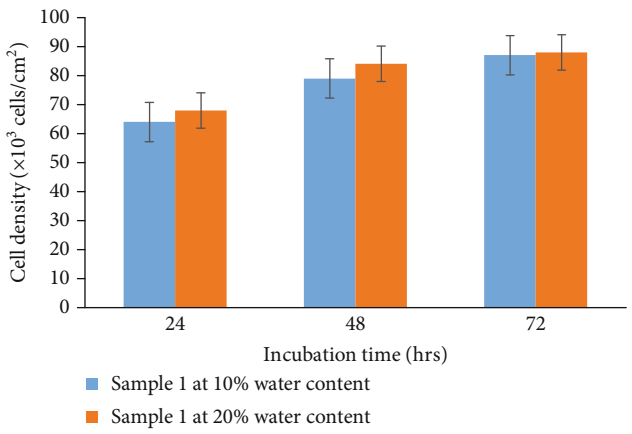

Figure 7: Cell count analysis of TiO_2 nanotubes fabricated under different water content levels.

was increased, and the sample was entirely covered with the cells. This function indicates that the sample was a nontoxic condition and encourages cell viability.

The increased development of osteoblast cells seen on a vertically aligned nanotube surface might be beneficial for additional applications, since it could be a pathway for increasing cell proliferation in a variety of different cell types. For therapeutic or diagnostic purposes, rare cells such as stem cells or pathogenic cells in small quantities may be grown at a faster rate. From the cell count of cell shown in Figure 6 indicates the incubation time of cells at 24, 48, and 72 hours. The black coloured bar indicates that (sample 1) nanotubes fabricated under the 10 vol. % of water content. Sample 2 indicates that 20 vol. % of water content added condition. From this cell count analysis, we could observe that 10 vol. % of water content nanotube fabrication samples deliver a lower cell count compared to the 20 vol % of water content at 24 hours of anodization. In 48 hours incubation time, the similar trend was observed. However, the 72 hours of incubation the samples deliver that nearly the same values could be identified from Figure 7. The increase in the cell growth with the increase in the incubation is credited to the increased length of the nanotube with the increase in the water content % [31].

4. Conclusion

TiO_2 nanotubes were successfully fabricated under 10 and 20 vol. % of water content added 5 minutes after the experiment begins. Two different surfaces of rib formations were achieved and identified by high resolution scanning electron microscope. The nanotube surface rib formation has been increased the nanomechanical properties were identified by nanoindentation analysis. The presence of ribs all over the nanotubes has highly supported the mechanical strength. Analysis of corrosion indicated the deposition of oxide film on the nanotubes had encouraged corrosion resistances. The long semicircle of the Nyquist plot indicates that the sample's resistivity on electrolyte medium was potentially increased after adding the water content in the anodization process. Moreover, the cell viability of the titanium material has been highly encouraged after 72 hours of incubation.

Data Availability

The data used to support the findings of this study are included in the article. Should further data or information be required, these are available from the corresponding author upon request.

Disclosure

It was performed as a part of the Employment of Mettu University, Ethiopia.

Conflicts of Interest

The authors declare that there are no conflicts of interest regarding the publication of this paper.

Acknowledgments

The authors thank Vellore Institute of Technology—Chennai and Saveetha School of Engineering, SIMATS—Chennai for providing characterization support to complete this research work.

References

[1] K. Gulati, K. Kant, D. Findlay, and D. Losic, "Periodically tailored titania nanotubes for enhanced drug loading and releasing performances," *Journal of Materials Chemistry B*, vol. 3, no. 12, pp. 2553–2559, 2015.

[2] Y. Y. Lu, Y. Y. Zhang, J. Zhang et al., "In situ loading of CuS nanoflowers on rutile TiO_2 surface and their improved photocatalytic performance," *Applied Surface Science*, vol. 370, pp. 312–319, 2016.

[3] C. Adán, J. Marugán, E. Sánchez, C. Pablos, and R. van Grieken, "Understanding the effect of morphology on the photocatalytic activity of TiO_2 nanotube array electrodes," *Electrochimica Acta*, vol. 191, pp. 521–529, 2016.

[4] V. Zwilling, E. Darque-Ceretti, A. Boutry-Forveille, D. David, M. Y. Perrin, and M. Aucouturier, "Structure and physicochemistry of anodic oxide films on titanium and TA6V alloy," *Surface and Interface Analysis*, vol. 27, no. 7, pp. 629–637, 1999.

[5] D. Gong, C. A. Grimes, O. K. Varghese et al., "Titanium oxide nanotube arrays prepared by anodic oxidation," *Journal of Materials Research*, vol. 16, no. 12, pp. 3331–3334, 2001.

[6] A. M. Vera-Jiménez, R. M. Melgoza-Alemán, M. G. Valladares-Cisneros, and C. Cuevas-Arteaga, "Synthesis and mechanical/-electrochemical characterization of TiO2 nanotubular structures obtained at high voltage," *Journal of Nanomaterials*, vol. 2015, Article ID 624073, 12 pages, 2015.

[7] K. Indira, U. K. Mudali, T. Nishimura, and N. Rajendran, "A review on TiO_2 nanotubes: influence of anodization parameters, formation mechanism, properties, corrosion behavior, and biomedical applications," *Journal of bio-and tribo-corrosion*, vol. 1, no. 4, pp. 1–22, 2015.

[8] V. Sivaprakash and R. Narayanan, "Surface modification TiO< sub>2</sub> nanotubes on titanium for biomedical application," *Materials Science Forum*, vol. 1019, pp. 157–163, 2021.

[9] S. Yogeshwaran, L. Natrayan, G. Udhayakumar, G. Godwin, and L. Yuvaraj, "Effect of waste tyre particles reinforcement on mechanical properties of jute and abaca fiber-epoxy hybrid composites with pre-treatment," *Materials Today: Proceedings*, vol. 37, no. 2, pp. 1377–1380, 2021.

[10] M. Kulkarni, A. Mazare, P. Schmuki, and A. Iglic, "Influence of anodization parameters on morphology of TiO2 nanostructured surfaces," *Advanced Materials Letters*, vol. 7, no. 1, pp. 23–28, 2016.

[11] V. Sivaprakash and R. Narayanan, "Anodic synthesis of TiO 2 nanotubes influence of water content and the analysis of the nano-mechanical application," *Journal of Bio-and Tribo-Corrosion*, vol. 6, no. 4, pp. 1–9, 2020.

[12] P. Roy, S. Berger, and P. Schmuki, "TiO2 nanotubes: synthesis and applications," *Angewandte Chemie International Edition*, vol. 50, no. 13, pp. 2904–2939, 2011.

[13] Z. Su, L. Zhang, F. Jiang, and M. Hong, "Formation of crystalline TiO_2 by anodic oxidation of titanium," *Progress in Natural Science: Materials International*, vol. 23, no. 3, pp. 294–301, 2013.

[14] E. Gilshtein, S. Pfeiffer, M. D. Rossell et al., "Millisecond photonic sintering of iron oxide doped alumina ceramic coatings," *Scientific Reports*, vol. 11, no. 1, pp. 1–10, 2021.

[15] P. Koking, O. Thumthan, and S. Noothongkaew, "Effect of DI water content on the growth of anatase TiO2 nanotubes synthesized by anodization process," in *Key engineering materials*, vol. 789, pp. 14–19, Trans tech publications ltd, 2018.

[16] J. M. Hernández-López, A. Conde, J. J. De Damborenea, and M. A. Arenas, "TiO2nanotubes with tunable morphologies," *RSC Advances*, vol. 4, no. 107, pp. 62576–62585, 2014.

[17] H. Yin, H. Liu, and W. Z. Shen, "The large diameter and fast growth of self-organized TiO2nanotube arrays achieved via electrochemical anodization," *Nanotechnology*, vol. 21, no. 3, p. 035601, 2010.

[18] K. Indira, U. Mudali, T. Nishimura, and N. Rajendran, "A review on TiO2 nanotubes: influence of anodization parameters, formation mechanism, properties, corrosion behavior, and biomedical applications," *Journal of Bio- and Tribo-Corrosion*, vol. 1, no. 4, 2015.

[19] D. Niu, A. Han, H. Cheng, S. Ma, M. Tian, and L. Liu, "Effects of organic solvents in anodization electrolytes on the morphology and tube-to-tube spacing of TiO_2 nanotubes," *Chemical Physics Letters*, vol. 735, p. 136776, 2019.

[20] K. Indira, U. K. Mudali, and N. Rajendran, "In-vitro biocompatibility and corrosion resistance of strontium incorporated TiO2 nanotube arrays for orthopaedic applications," *Journal of Biomaterials Applications*, vol. 29, no. 1, pp. 113–129, 2014.

[21] A. Muñoz-Mizuno, M. Cely-Bautista, J. Jaramillo-Colpas, D. Hincapie, and J. W. Calderón-Hernández, "Effect on thermal oxidation in TiO2 nanostructures on nanohardness and corrosion resistance," *Ingeniare*, vol. 28, no. 3, pp. 362–372, 2020.

[22] R. Kashkovskiy, K. Strelnikova, and A. Fedotova, "Application of electrochemical impedance spectroscopy to study hydrogen sulphide corrosion of steel and its inhibition: a review," *Corrosion Engineering, Science and Technology*, vol. 54, no. 6, pp. 493–515, 2019.

[23] K. Indira, U. Kamachi Mudali, and N. Rajendran, "In vitro bioactivity and corrosion resistance of Zr incorporated TiO_2 nanotube arrays for orthopaedic applications," *Applied Surface Science*, vol. 316, pp. 264–275, 2014.

[24] J. F. Gómez-Aguilar, J. E. Escalante-Martínez, C. Calderón-Ramón, L. J. Morales-Mendoza, M. Benavidez-Cruz, and M. Gonzalez-Lee, "Equivalent circuits applied in electrochemical impedance spectroscopy and fractional derivatives with and without singular kernel," *Advances in Mathematical Physics*, vol. 2016, Article ID 9720181, 15 pages, 2016.

[25] K. T. Arul, E. Manikandan, J. R. Ramya et al., "Enhanced anticorrosion properties of nitrogen ions modified polyvinyl alcohol/Mg-Ag ions co-incorporated calcium phosphate coatings," *Materials Chemistry and Physics*, vol. 261, p. 124182, 2021.

[26] Y. Huang, Z. Xu, X. Zhang et al., "Nanotube-formed Ti substrates coated with silicate/silver co-doped hydroxyapatite as prospective materials for bone implants," *Journal of Alloys and Compounds*, vol. 697, pp. 182–199, 2017.

[27] V. Sivaprakash and R. Narayanan, "Synthesis of TiO_2 nanotubes via electrochemical anodization with different water content," *Materials Today: Proceedings*, vol. 37, pp. 142–146, 2021.

[28] H. Uzal and A. Döner, "Corrosion behavior of titanium dioxide nanotubes in alkaline solution," *Protection of Metals and Physical Chemistry of Surfaces*, vol. 56, no. 2, pp. 311–319, 2020.

[29] R. Hang, Y. Liu, L. Zhao et al., "Fabrication of Ni-Ti-O nanotube arrays by anodization of NiTi alloy and their potential applications," *Scientific Reports*, vol. 4, no. 1, pp. 21–24, 2015.

[30] R. Yew, S. K. Karuturi, J. Liu, H. H. Tan, Y. Wu, and C. Jagadish, "Exploiting defects in TiO2inverse opal for enhanced photoelectrochemical water splitting," *Optics Express*, vol. 27, no. 2, p. 761, 2019.

[31] S. Oh, C. Daraio, L. H. Chen, T. R. Pisanic, R. R. Finones, and S. Jin, "Significantly accelerated osteoblast cell growth on aligned TiO2 nanotubes," *Journal of Biomedical Materials Research Part A*, vol. 78, no. 1, pp. 97–103, 2006.